



CHAPTER IV

ELECTROSPINNING OF HEXANOYL CHITOSAN

4.1 Abstract

Ultrafine hexanoyl chitosan (H-chitosan) fibers were successfully prepared by electrospinning of hexanoyl chitosan solutions in chloroform. The concentration of the spinning solutions was between 4% and 14% w/v. The as-spun fibers appeared to be flat with ribbonlike morphology and exhibited average diameters in the range of 0.64–3.93 μm . With increasing H-chitosan concentration, the average fiber diameter was found to increase, while the bead density was found to decrease. An increase in the applied electrical potential was responsible for increasing the average diameter of the as-spun fibers. Finally, the addition of an organic salt, pyridinium formate, helped increase the conductivity of the spinning solution, which resulted in a general increase in the average diameter and a general decrease in the bead density of the resulting H-chitosan fibers.

(**Keywords:** Electrospinning; Chitosan derivative; Ultrafine fiber)

4.2 Introduction

In recent years, much attention has been paid to the use of high electrical potentials in fabricating ultrafine fibers from materials of diverse origins, a process known as electrostatic spinning or electrospinning, with diameters being in sub-micron down to nanometer range (Frenot & Chronakis, 2003; Huang, Zhang, Kotaki, & Ramakrishna, 2003; Li & Xia, 2004). This process involves the application of a strong electrostatic field over a conductive capillary attaching to a reservoir containing a polymer solution or melt and a conductive collection screen. Upon increasing the electrostatic field strength up to but not exceeding a critical value, charge species accumulated on the surface of a pendant drop destabilize the hemispherical shape into a conical shape (commonly known as Taylor's cone). Beyond the critical value, a charged polymer jet is ejected from the apex of the cone

(as a way of relieving the charge built-up on the surface of the pendant drop). The ejected charged jet is then carried to the collection screen via the electrostatic force. The Coulombic repulsion force is responsible for the thinning of the charged jet during its trajectory to the collection screen. The thinning down of the charged jet is limited by the viscosity increase as the charged jet is dried. Recently, in an attempt to mimic natural tissue *in vitro*, the technique of electrospinning has been reestablished due mainly to its potential to fabricate fibrous structure with which diameters in the range close to the collagen fibers found in the natural extracellular matrix (ECM) of about 30–130 nm (Matthews, Wnek, Simpson, & Bowlin, 2002). Because of the great expectations for utilizing electrospun fibers in biomedical applications, a number of natural and synthetic biodegradable polymers have been electrospun: they are, for examples, native collagens from calfskin (type I) and human placenta (types I and III) (Matthews et al., 2002), bovine fibrinogen fraction I (Wnek, Carr, Simpson, & Bowlin, 2003), Bombyx mori and Samia Cynthia ricini silk fibroins (Ohgo, Zhao, Kobayashi, & Asakura, 2003), dextran, methacrylated dextran, and dextran/ poly(D,L-lactide-co-glycolide) (PLGA) hybrids (Jiang, Fang, Hsiao, Chu, & Chen, 2004), poly(ester urethane)urea (PEUU)/bovine collagen type I hybrids (Stankus, Guan, & Wagner, 2004), and PLGA/chitin hybrids (Min, You, Kim, Lee, & Park, 2004a). Chitosan or poly(N-acetyl-D-glucosamine-co-D-glucosamine) is a partially N-deacetylated derivative of chitin or poly(N-acetyl-D-glucosamine), which is one of the most abundant polysaccharides commonly found in shells of various insects and crustaceans as well as cell walls of various fungi. Even though chitin has structural characteristics similar to glycosaminoglycans (GAGs), such as chondroitin sulfate and hyaluronic acid in the ECM (Muzzareli, 1985), its utilization is somewhat limited by its poor solubility and reactivity and its physical properties that are rigid and brittle, a direct result of strong intra- and inter-molecular hydrogen bonding. Chitosan has been explored as a suitable functional material for biomedical utilization, mainly due to its biocompatibility, biodegradability, and non-toxicity (Ravi Kumar, 2000). Electrospinning of pure chitosan has proven to be quite difficult (Duan, Dong, Yuan, & Yao, 2004; Ohkawa, Cha, Kim, Nishida, & Yamamoto, 2004; Park, Jeong, Yoo, & Hudson, 2004; Spasova, Manolova, Paneva, & Rashkov, 2004), therefore early reports on

electrospun chitosan fibers have been in blends with other spinnable polymers, such as poly(ethylene oxide) (PEO) in an aqueous solution of acetic acid (Duan et al., 2004) and in water (Spasova et al., 2004), silk fibroin in aqueous solution of formic acid (Park et al., 2004), and poly(vinyl alcohol) (PVA) in aqueous solutions of formic acid (Ohkawa et al., 2004). Successful preparation of electrospun chitosan fibers has recently been reported from chitosan solutions in trifluoroacetic acid (TFA) (Ohkawa et al., 2004) and from deacetylation of electrospun chitin fibers from chitin solutions in 1,1,1,3,3,3-hexafluoro-2-propanol (HFIP) (Min et al., 2004b). Despite the reported success in the preparation of electrospun chitosan fibers, their actual use may be limited by the cost and toxicity of TFA and HFIP. An alternative approach is chemical modifications of chitosan into derivatives that are soluble in a wide variety of common organic solvents. Organically soluble derivatives of chitosan can be used to formulate materials for biomedical applications such as polymeric drugs and artificial organs with high specificity and wide applicability. Among such derivatives, acylated chitosans are soluble in various common organic solvents, such as chloroform, benzene, pyridine, and tetrahydrofuran (THF) (Zong, Kimura, Takahashi, & Yamane, 2000). Among various acylated chitosans, hexanoyl chitosan (H-chitosan) was found to be anti-thrombogenic and resistant to hydrolysis by lysosome (Hirano & Noishiki, 1985; Lee, Ha, & Park, 1995). As a result, H-chitosan is a very interesting derivative of chitosan for use in biomedical applications. In the present contribution, successful preparation of H-chitosan electrospun fibers from H-chitosan solutions in chloroform was reported for the first time. Effects of H-chitosan concentration, applied electrical potential, and organic salt addition on the morphological appearance of the as-spun H-chitosan fibers were investigated.

4.3 Experimental

4.3.1 Materials

Chitosan was prepared from shells of *Penaeus merguensis* shrimps [Surapon Foods Public Co., Ltd. (Thailand)]. The degree of deacetylation (DD) of the as-prepared chitosan was determined based on an infrared spectroscopic method (Sabnis & Block, 1997) to be about 88%, while the viscosity-average molecular

weight \overline{M}_v was evaluated from the intrinsic viscosity $[\eta]$ based on the Mark–Houwink equation ($[\eta] = K\overline{M}_v^a$, where K and a are constants which, for chitosan, they were determined to be 6.59×10^{-3} ml/g and 0.88 (Wang, Bo, Li, & Qin, 1991), respectively) to be about 5.76×10^{-3} g/mol. The intrinsic viscosity was measured in a mixture of 0.2 M acetic acid and 0.1 M sodium acetate at 30 °C. Hexanoyl chloride or caproyl chloride (Fluka, France), formic acid (Merck, USA), and methanol (Labsan Asia, Thailand) were used as received. Pyridine and chloroform (Labsan Asia, Thailand) were distilled and dried over molecular sieve prior to further use. All chemicals were of analytical reagent grade.

4.3.2 Preparation of Hexanoyl Chitosan

Hexanoyl chitosan (H-chitosan) was prepared by a heterogeneous acylation reaction of the as-prepared chitosan with hexanoyl chloride based on the method described by Zong et al. (2000) (see Figure 4.1 for chemical structures of chitosan and H-chitosan shown with full substitution of hexanoyl groups). In each synthesis batch, about 3.2 g of the as-prepared chitosan powder ($\leq 60 \mu\text{m}$) was soaked in pyridine for one week, after which pyridine was evaporated under a reduced pressure. The chitosan was further soaked in a mixture of pyridine and chloroform (90 ml of pyridine and 45 ml of chloroform) for one day. The mixture was cooled to about -10 to -5 °C in an ice-salt bath. About 21.2 ml of hexanoyl chloride dissolved in chloroform was later added dropwise to the mixture within 2 h. The mixture was further stirred at room temperature for 2 h and then refluxed at 98 °C for another 6 h. The fully reacted mixture was poured into 300 ml of methanol and the precipitate was filtered, dissolved in chloroform, and re-precipitated in methanol. The re-precipitation was repeated four times. Light yellowish H-chitosan product was finally obtained after the precipitated product had been dried in vacuo at room temperature overnight.

4.3.3 Electrospinning of Hexanoyl Chitosan

H-chitosan spinning dopes were prepared by dissolving a weighed amount of the as-synthesized H-chitosan product in a measured quantity of chloroform to produce H-chitosan solutions with concentrations ranging between 4% and 14% w/v. Due to incomplete dissolution, H-chitosan solutions with

concentrations greater than 14% w/v could not be prepared. These solutions of varying concentration were used to investigate the effect of H-chitosan concentration on morphology of the as-spun H-chitosan fibers. To study the effect of organic salt addition, pyridinium formate (PF), prepared by reacting pyridine and formic acid in an equimolar amount, in varying amount ranging from 2.5% to 10% w/v was added to 8% w/v H-chitosan solution in chloroform. PF was added to increase the conductivity of the spinning dope. The schematic diagram for the electrospinning setup is illustrated in Figure 4.2. About 3 ml of a H-chitosan solution was put in a 5-ml syringe, with a blunt-end, stainless steel needle (inner diameter = 0.9 mm) being attached at the open end. Both the syringe and the needle was tilted 45° from a vertical line. The needle was connected to the emitting electrode of a Gamma High Voltage Research ES30P-5W high-voltage supply capable of generating DC voltages in the range of 0–30 kV. An aluminum foil, used as the collection screen, was connected to the ground electrode of the power supply and was placed perpendicular to the needle. The distance between the needle tip and the collection screen defines a collection distance. The applied electrical potential was between 8 and 18 kV and the collection distance was fixed at 12 cm. The electrospinning process was carried out at room temperature (i.e., about 25 °C).

4.3.4 Characterization

The successful hexanoylation of chitosan to obtain H-chitosan was confirmed by a Thermo Nicolet Nexus 670 Fourier-transformed infrared spectrometer (FT-IR) using KBr pellet method and a Bruker Mercury Variant 400 MHz proton-nuclear magnetic resonance spectrometer (¹H-NMR) using deuterated chloroform as the solvent, while the degree of substitution (DS) of hexanoyl groups on H-chitosan molecules was determined by a Perkin-Elmer PE2400 series II elemental analyzer (EA). Shear viscosity, conductivity, and surface tension of the as-prepared solutions were measured by a Brookfield DV-III programmable viscometer, a Orion 160 conductivity meter, and a KRÜSS DSA10-Mk2 drop-shape analyzer, respectively, at 25 °C. Morphological appearance of the as-spun products was examined by a JEOL JSM-5200 scanning electron microscope (SEM). Each sample was coated with thin layer of gold using a JEOL JFC-1100E ion sputtering device prior to observation under SEM. Diameters of the as-spun fibers were measured

directly from SEM images, with the average value being calculated from at least 50 measurements (for each spinning condition). The average number of beads per unit area (i.e., the bead density) on the as-spun beaded fibers was calculated from measurements on SEM images of 100x magnification. JOEL SemAfore 4.0 and SPSS 11.0 PC programs were used to obtain the statistical values of the measurements.

4.4 Results and Discussion

4.4.1 Characterization of Hexanoyl Chitosan

IR spectra of the original chitosan and the as-synthesized hexanoyl chitosan (H-chitosan) are shown in Figure 4.3. The broad absorption peak at 3000–3700 cm^{-1} (OH, NH₂) was evident in the spectra of both chitosan and H-chitosan. This indicates that hexanoyl groups did not fully substitute into all of the hydroxyl and amine groups on chitosan molecules. In addition to the absorption peaks observed for chitosan, additional peaks were observed in the IR spectrum of H-chitosan: they are 1716 cm^{-1} (C=O of NCOR) and 1751 cm^{-1} (C=O of OCOR), corresponding to the substitution of hexanoyl groups at amine and hydroxyl groups of chitosan, respectively. Figure 4.4 shows ¹H-NMR spectrum of H-chitosan in deuterated chloroform. The spectrum obtained was similar to that reported by Zong et al. (2000). Specifically, the as-synthesized H-chitosan showed signals at 5.7 (H1), 5.3 (H3), 4.3 (H4), 3.3 to 3.8 (H6, H5), 2.7 (H2) ppm, corresponding to the protons attaching to carbons on the polysaccharide ring, and signals at 2.4 (Ha), 1.2 to 1.8 (Hb), and 0.9 (Hc) ppm, belonging to the protons attaching to carbons on hexanoyl side chains. Lastly, the EA result showed that the DS of hexanoyl groups on chitosan molecules was about 3.0 (i.e., Calcd: C, 63.23; H, 8.96; N, 3.04. Found: C, 63.23; H, 9.17; N, 3.00). It should be noted that the DS for fully substituted H-chitosan is 4.0 (Zong et al., 2000).

4.4.2 Electrospinning of Hexanoyl Chitosan

To observe the effect of H-chitosan concentration on morphological appearance of the as-spun products, H-chitosan solutions with concentrations ranging from 4% to 14% w/v were prepared. Table 4.1 summarizes some properties of the as-

prepared solutions. Both viscosity and conductivity of the solutions increased, while surface tension decreased very slightly, with increasing H-chitosan concentration. The increase in the viscosity can be attributed to increased chain entanglement (Mit-uppatham, Nithitanakul, & Supaphol, 2004a; Mit-uppatham, Nithitanakul, & Supaphol, 2004b; Wannatong, Sirivat, & Supaphol, 2004) and the increase in the conductivity could be due to the increased in the free hydroxyl groups on H-chitosan molecules, while the decrease in the surface tension could be attributed to the decrease in the cohesiveness of chloroform molecules at the air–liquid interface due to the presence of H-chitosan molecules. Generally, a critical concentration is needed to be exceeded in order to obtain fibers from electrospinning. Below this concentration, chain entanglements are insufficient to stabilize the Coulombic repulsion within the ejected jet, leading to formation of sprayed droplets (Mituppatham et al., 2004a, 2004b; Wannatong et al., 2004). SEM images of as-spun products from H-chitosan solutions in chloroform with varying concentration are illustrated in Fig. 4.5. It should be noted that these products were spun under a fixed applied electrical field strength of 12 kV/12 cm. Clearly, beads with only a small proportion of fibers were observed from the solution with the lowest concentration investigated (4% w/v). With a slight increase in the H-chitosan concentration to 6% w/v, a combination of both beads and beaded fibers was observed. Further increase in the H-chitosan concentration increased fiber formation, at the expense of bead formation and, at the highest concentration investigated (14% w/v), only fibers were formed. Interestingly, the as-spun fibers appeared to be ribbon-like, most likely a result of the rapid evaporation of chloroform [boiling point = 61 °C and vapour pressure = 159 mmHg at 20 °C (Tidwell, 2006)] during their flight to the collective target. Due to the ribbon-like nature of the as-spun fibers, the measurement for the size of the as-spun fibers went by their width. It should be noted that, for this particular case, the words ‘diameter’ and ‘width’ were used synonymously. The average diameter and the bead density of the as-spun fibers are summarized in Table 4.1. The average fiber diameter increased from about 0.64 μm at the concentration of 6% w/v to about 3.93 μm at the concentration of 14% w/v. On the contrary, the bead density decreased from about 2.13×10^5 beads/ cm^2 at the concentration of 6% w/v to about 3.48×10^4 beads/ cm^2 at the concentration of 10% w/v. The increase in the

fiber diameter with increasing H-chitosan concentration should be a result of the increased viscoelastic force that works against the Coulombic repulsion force and the decreased path length of the charged jet that reduces the on-flight time during which a charged jet segment is thinned down by the Coulombic repulsion force (Mit-uppatham et al., 2004a, 2004b; Wannatong et al., 2004). To observe the effect of applied electrical potential on morphological appearance of the as-spun fibers, 8% w/v H-chitosan solution in chloroform was spun under an applied electrical potential in the range of 8–18 kV over a fixed collection distance of 12 cm. The average diameter of the as-spun H-chitosan fibers for each spinning condition is summarized in Table 4.2. Apparently, the average fiber diameter increased slightly with increasing applied electrical potential. Specifically, the average diameter increased from about 1.02 μm at the applied electrical potential of 8 kV to about 1.32 μm at the applied electrical potential of 18 kV. The observed increase in the average fiber diameter could be a result of the increase in the electrostatic force that causes both the reduction in the path length and the increase in the mass throughput (Mit-uppatham et al., 2004a, 2004b; Wannatong et al., 2004). To observe the effect of conductivity on morphological appearance of the as-spun fibers, 8% w/v H-chitosan solution in chloroform was spun with the addition of pyridinium formate salt (PF) in varying amount ranging between 0% and 10% w/v under a fixed applied electrical field strength of 12 kV/12 cm. Advantages of PF are twofold: (1) PF is an organic salt which is soluble in a wide variety of organic solvents and (2) PF is volatile so the as-spun fibers are free from this chemical. Table 4.3 summarizes the conductivity value of the resulting H-chitosan solution as well as average diameter and bead density of the as-spun H-chitosan fibers. Evidently, conductivity of the solution increased markedly on the addition of PF. The average fiber diameter was, in general, found to increase with increasing conductivity of the solution, most likely a result of the increased mass throughput due to the increase in the electrostatic force (Mit-uppatham et al., 2004a, 2004b; Wannatong et al., 2004). The increase in the Coulombic repulsion, on the other hand, was responsible for the observed decrease in the bead density of the as-spun H-chitosan fibers. Figure 4.6 shows morphological appearance of as-spun H-chitosan fibers from a solution containing 8% w/v H-chitosan with and without the addition of 7.5% w/v PF. Clearly, the obtained fibers

appeared to be ribbon-like, but the fibers obtained from the solution with the addition of PF showed a much lower proportion of beads in comparison with those obtained from the solution without PF. In addition to the ribbon-like morphology of the as-spun fibers, SEM images of higher magnifications revealed that the surface of as-spun PF-free H-chitosan fibers was rough with minute pores being present on it (see Figure 4.7a). The surface of as-spun PF-added H-chitosan fibers was also rough, but without the presence of minute pores (see Figure 4.7b). It is postulated that the formation of minute pores on the surface of the as-spun PF-free H-chitosan fibers could be due to local phase separation and low boiling point of chloroform that, after evaporation of chloroform, resulted in the chloroform-rich phase to become minute pores. The exact mechanism, however, is still unclear (Casper, Stephens, Tassi, Chase, & Rabolt, 2004).

4.5 Conclusions

Electrospun hexanoyl chitosan (H-chitosan) fibers with ribbon-like morphology and average diameters ranging from 0.64 to 3.93 μm were successfully prepared from solutions of H-chitosan in chloroform. The concentration range investigated was between 4% and 14% w/v. With increasing H-chitosan concentration, the average fiber diameter was found to increase, while the bead density was found to decrease. An increase in the applied electrical potential was responsible for increasing the average diameter of the as-spun fibers. Finally, addition of an organic salt, pyridinium formate, helped increase the conductivity of the spinning solution, which resulted in a general increase in the average diameter and a general decrease in the bead density of the resulting H-chitosan fibers.

4.6 Acknowledgments

This work was supported in part by (1) the National Research Council of Thailand, (2) Chulalongkorn University (through invention and research grants from the Ratchadapesek Somphot Endowment Fund), (3) the Petroleum and Petrochemical Technology Consortium [through a Thai governmental loan from the Asian

Development Bank (ADB)], and (4) the Petroleum and Petrochemical College (PPC), Chulalongkorn University. A. Neamnark acknowledges a doctoral scholarship received from the Royal Golden Jubilee PhD Program, the Thailand Research Fund (TRF). Lastly, Patcharaporn Wutticharoenmongkol is acknowledged for her assistance on SEM observation.

4.7 References

- Casper, C. L., Stephens, J. S., Tassi, N. G., Chase, D. B., & Rabolt, J. F. (2004). Controlling surface morphology of electrospun polystyrene fibers: effect of humidity and molecular weight in the electrospinning process. *Macromolecules*, 37, 573–578.
- Duan, B., Dong, C., Yuan, X., & Yao, K. (2004). Electrospinning of chitosan solutions in acetic acid with poly(ethylene oxide). *Journal of Biomaterials Science – Polymer Edition*, 15, 797–811.
- Frenot, A., & Chronakis, I. S. (2003). Polymer nanofibers assembled by electrospinning. *Current Opinion in Colloid and Interface Science*, 8, 64–75.
- Hirano, S., & Noishiki, Y. (1985). The blood compatibility of chitosan and N-acetylchitosans. *Journal of Biomedical Materials Research*, 19, 413–417.
- Huang, Z. M., Zhang, Y. Z., Kotaki, M., & Ramakrishna, S. (2003). A review on polymer nanofibers by electrospinning and their applications in nanocomposites. *Composite Science and Technology*, 63, 2223–2253.
- Jiang, H., Fang, D., Hsiao, B. S., Chu, B., & Chen, W. (2004). Optimization and characterization of dextran membranes prepared by electrospinning. *Biomacromolecules*, 5, 326–333.
- Lee, K. Y., Ha, W. S., & Park, W. H. (1995). Blood compatibility and biodegradability of partially N-acetylated chitosan derivatives. *Biomaterials*, 16, 1211–1216.
- Li, D., & Xia, Y. (2004). Electrospinning of nanofibers: reinventing the wheel?. *Advanced Materials* 16, 1151–1170.

- Matthews, J. A., Wnek, G. E., Simpson, D. G., & Bowlin, G. L. (2002). Electrospinning of collagen nanofibers. *Biomacromolecules*, 3, 232–238.
- Min, B. M., You, Y., Kim, J. M., Lee, S. J., & Park, W. H. (2004a). Formation of nanostructured poly(lactic-co-glycolic acid)/chitin matrix and its cellular response to normal human keratinocytes and fibroblasts. *Carbohydrate Polymers*, 57, 285–292.
- Min, B. M., Lee, S. W., Lim, J. N., You, Y., Lee, T. S., Kang, P. H., et al. (2004b). Chitin and chitosan nanofibers: electrospinning of chitin and deacetylation of chitin nanofibers. *Polymer*, 45, 7137–7142.
- Mit-uppatham, C., Nithitanakul, M., & Supaphol, P. (2004a). Effects of solution concentration, emitting electrode polarity, solvent type, and salt addition on electrospun polyamide-6 fibers: a preliminary report. *Macromolecular Symposia*, 216, 293–299.
- Mit-uppatham, C., Nithitanakul, M., & Supaphol, P. (2004b). Ultrafine electrospun polyamide-6 fibers: effect of solution condition on morphology and average fiber diameter. *Macromolecular Chemistry and Physics*, 205, 2327–2338.
- Muzzareli, R. A. A. (1985). In *Encyclopedia of polymer science and engineering* (3rd ed., pp. 430–440). New York, USA: Wiley & Sons.
- Ohgo, K., Zhao, C., Kobayashi, M., & Asakura, T. (2003). Preparation of non-woven nanofibers of *Bombyx mori* silk, *Samia cynthia ricini* silk and recombinant hybrid silk with electrospinning method. *Polymer*, 44, 841–846.
- Ohkawa, K., Cha, D., Kim, H., Nishida, A., & Yamamoto, H. (2004). Electrospinning of chitosan. *Macromolecular Rapid Communications*, 25, 1600–1605.
- Park, W. H., Jeong, L., Yoo, D. I., & Hudson, S. (2004). Effect of chitosan on morphology and conformation of electrospun silk fibroin nanofibers. *Polymer*, 45, 7151–7157.
- Ravi Kumar, M. N. V. (2000). A review of chitin and chitosan applications. *Reactive and Functional Polymers*, 46, 1–27.
- Sabnis, S., & Block, L. H. (1997). Improved infrared spectroscopic method for the analysis of degree of N-deacetylation of chitosan. *Polymer Bulletin*, 39, 67–71.

- Spasova, M., Manolova, N., Paneva, D., & Rashkov, L. (2004). Preparation of chitosan-containing nanofibres by electrospinning of chitosan/poly(ethylene oxide) blend solutions. *e-Polymers*, Art. No. 056.
- Stankus, J. J., Guan, J., & Wagner, W. R. (2004). Fabrication of biodegradable elastomeric scaffolds with sub-micron morphologies. *Journal of Biomedical Materials Research*, 70A, 603–614.
- Tidwell, J. (2006). Safety Data For Chloroform. <<http://allergies.about.com/library/chem/blmsds-chloroform.htm>>.
- Wang, W., Bo, S., Li, S., & Qin, W. (1991). Determination of the Mark–Houwink equation for chitosans with different degrees of deacetylation. *International Journal of Biological Macromolecules*, 13, 281–285.
- Wannatong, L., Sirivat, A., & Supaphol, P. (2004). Effects of solvents on electrospun polymeric fibers: preliminary study on polystyrene. *Polymer International*, 53, 1851–1859.
- Wnek, G. E., Carr, M. E., Simpson, D. G., & Bowlin, G. L. (2003). Electrospinning of nanofiber fibrinogen structures. *Nano Letters*, 3, 213–216.
- Zong, Z., Kimura, Y., Takahashi, M., & Yamane, H. (2000). Characterization of chemical and solid state structures of acylated chitosans. *Polymer*, 41, 899–906.

Table 4.1 Viscosity, conductivity, surface tension of hexanoyl chitosan solutions in chloroform and observed average diameter and bead density of as-spun hexanoyl chitosan fibers. The applied electrostatic field strength was 12 kV/12 cm

Concentration of H-chitosan solution (% w/v)	Viscosity ^a (cp)	Conductivity ($\mu\text{S/cm}$)	Surface tension (mN/m)	Average fiber diameter (μm)	Bead density (beads/cm ²)
4	16.4	0.25	27.2	n/a ^b	n/a ^b
6	49.0	0.27	26.8	0.64 \pm 0.36	2.13 $\times 10^5$
8	104	0.28	26.1	1.23 \pm 0.67	1.51 $\times 10^5$
10	193	0.35	25.4	1.49 \pm 0.69	3.48 $\times 10^4$
14	956	0.40	25.6	3.93 \pm 1.82	0

The applied electrostatic field strength was 12 kV/12 cm.

a The shear rates associated with the viscosity measurement were 233 round/s for 4–10% w/v H-chitosan solutions and 47 round/s for 14% w/v H-chitosan solution.

b Only beads were observed for this concentration.

Table 4.2 Average diameter of as-spun hexanoyl chitosan fiber from 8% w/v hexanoyl chitosan solution in chloroform as a function of varying applied electric potential ranging between 8 and 18 kV over a fixed collection distance of 12 cm

Applied electric potential (kV)	Average fiber diameter (μm)
8	1.02 ± 0.62
10	1.22 ± 0.63
12	1.23 ± 0.67
14	1.26 ± 0.64
16	1.27 ± 0.67
18	1.32 ± 0.65

Table 4.3 Conductivity of 8% w/v hexanoyl chitosan solution in chloroform with addition of pyridinium formate in varying amount ranging between 0 and 10.0% w/v and observed average diameter, bead density, and observed average diameter to bead density ratio of as-spun hexanoyl chitosan fibers. The applied electrostatic field strength was 12 kV/12 cm

Pyridinium formate content (% w/v)	Conductivity ($\mu\text{S/cm}$)	Average fiber diameter (μm)	Bead density (beads/cm ²)
0	0.28	1.23 \pm 0.67	1.51 \times 10 ⁵
2.5	1.20	1.31 \pm 0.74	5.24 \times 10 ⁴
5.0	1.90	1.29 \pm 0.75	3.70 \times 10 ⁴
7.5	3.84	1.49 \pm 0.65	3.34 \times 10 ⁴
10.0	7.90	0.93 \pm 0.54	1.68 \times 10 ⁴

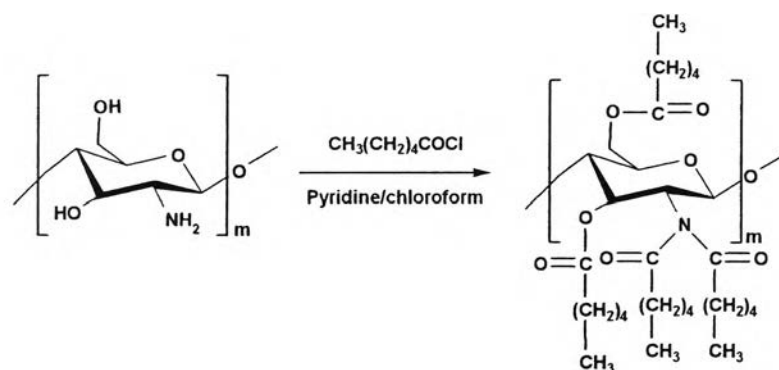


Figure 4.1 A synthetic route for perfect hexanoyl chitosan.

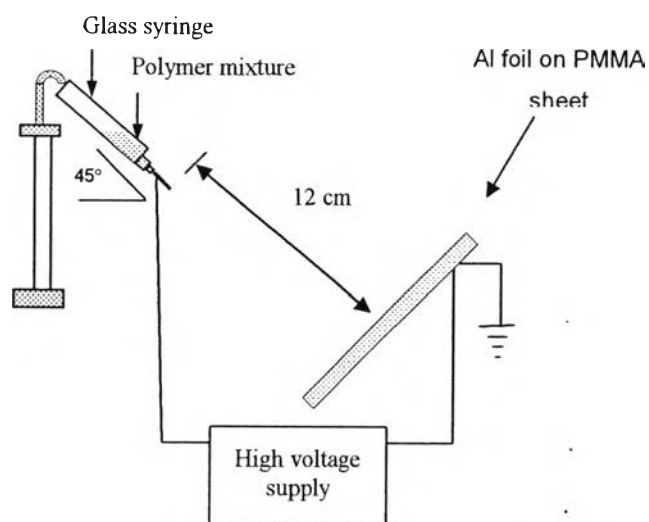


Figure 4.2 Schematic diagram of electrospinning set-up device.

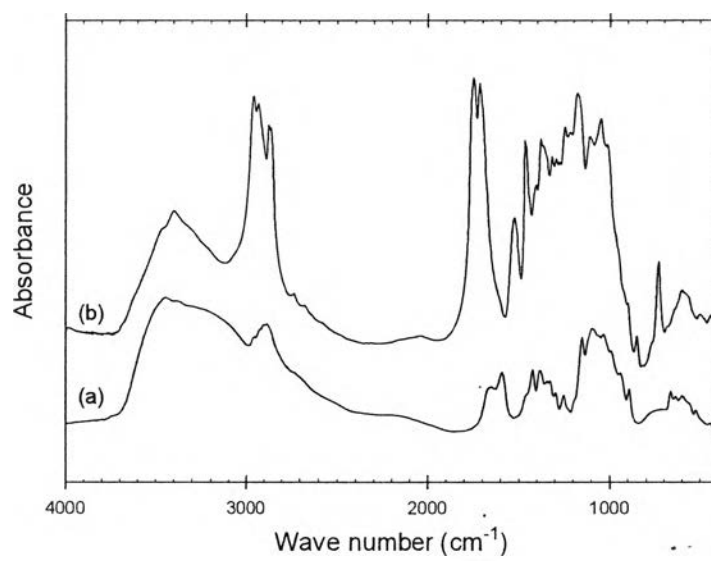


Figure 4.3 IR spectra of (a) chitosan and (b) hexanoyl chitosan.

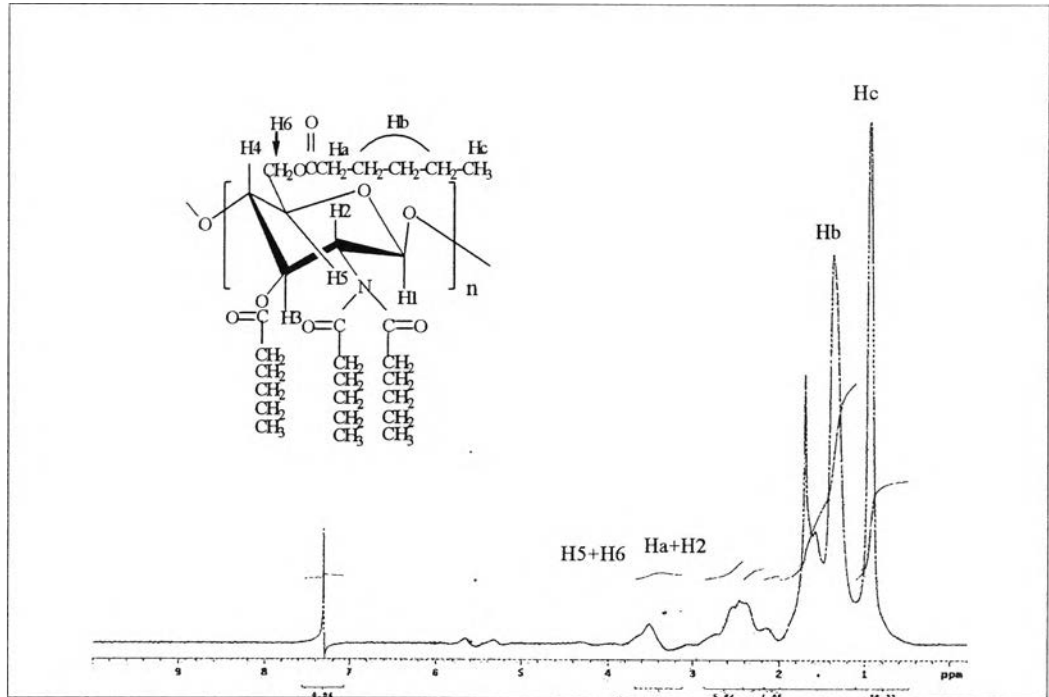


Figure 4.4 $^1\text{H-NMR}$ spectrum of hexanoyl chitosan in deuterated chloroform.

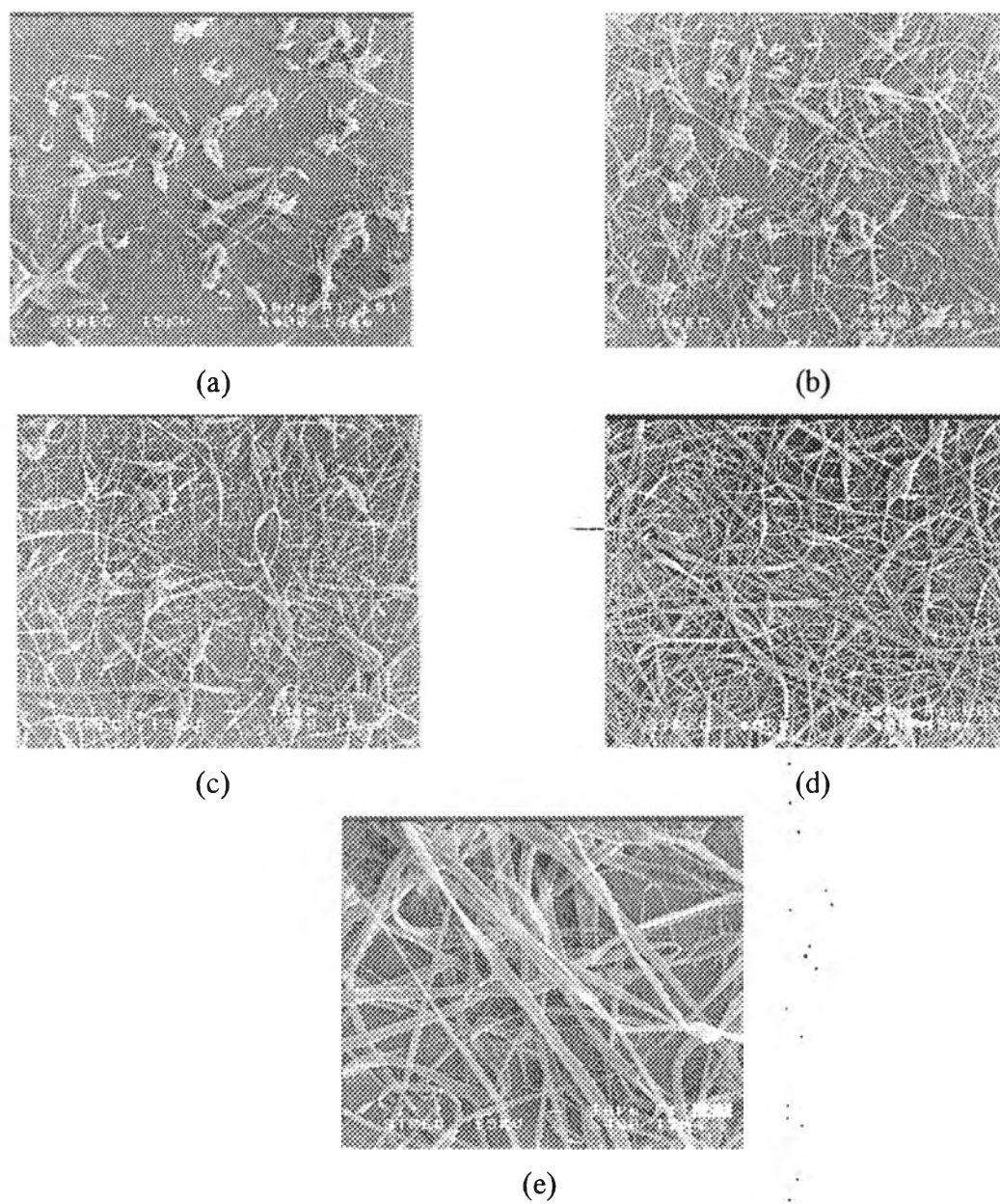
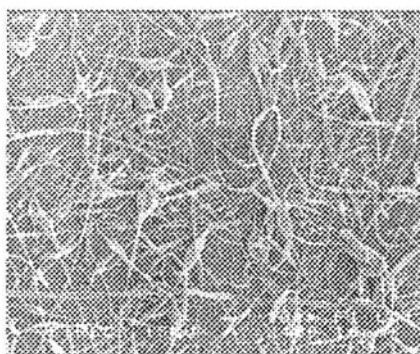
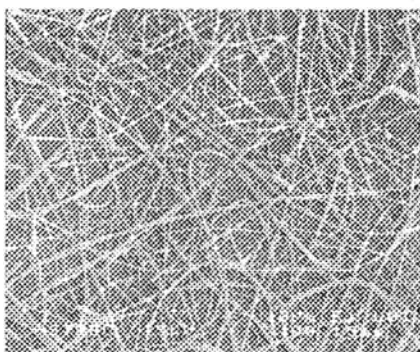


Figure 4.5 SEM images of as-spun products from (a) 4, (b) 6, (c) 8, (d) 10, and (e) 14% (w/v) hexanoyl chitosan solutions in chloroform (magnification = 400x and scale bar = 10 μm). The applied electric field strength was 12 kV/12 cm.

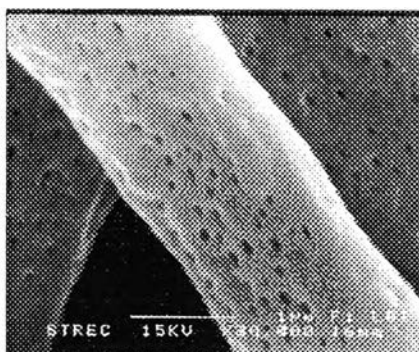


(a)

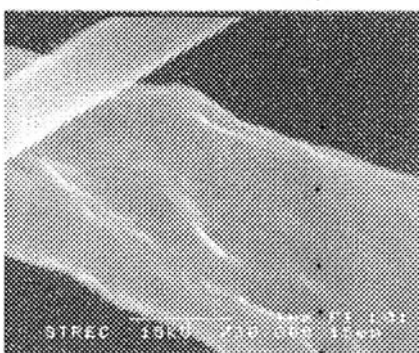


(b)

Figure 4.6 SEM images of as-spun fibers from 8% w/v hexanoyl chitosan solution in chloroform (a) without addition of pyridinium formate salt and (b) with 7.5% w/v pyridinium formate salt addition (magnification = 400x and scale bar = 10 μm). The applied electric field strength was 12 kV/12 cm.



(a)



(b)

Figure 4.7 Surface morphology of the as-spun fibers 8% w/v hexanoyl chitosan solution in chloroform (a) without addition of pyridinium formate salt and (b) with 7.5% w/v pyridinium formate salt addition (magnification = 30000x and scale bar = 1 μ m). The applied electric field strength was 12 kV/12 cm.